Geotechnical aspect of the damage caused by the April 25th, 2015 Gorkha earthquake of Nepal

Kazuo KONAGAI[1], Rama Mohan POKHREL[2], Hitoshi MATSUBARA[3] and Masataka SHIGA[4]

[1]Fellow of JSCE, Professor, Graduate School of Urban Innovation, Yokohama National University
(Tokiwadai 79-1, Hodogaya-ku, Yokohama 240-8501, Japan)
E-mail:konagai@ynu.ac.jp
[2] Member of JSCE, JSPS Research Fellow, Institute of Industrial Science, University of Tokyo
(Komaba 4-6-1, Meguro-ku, Tokyo 153-8505, Japan)
E-mail: pokhrel@iis.u-tokyo.ac.jp
[3]Member of JSCE, Associate Professor, Faculty of Engineering, University of the Ryukyu
(Senbaru 1, Nishihara-cho, Okinawa 903-0213. Japan)
E-mail: matsbara@tec.u-ryukyu.ac.jp
[4]Undergraduate student, Department of Civil Engineering, Yokohama National University
(Tokiwadai 79-1, Hodogaya-ku, Yokohama 240-8501, Japan)
E-mail: shiga-masataka-ft@ynu.jp

Key Facts
- Hazard Type: Earthquake
- Date of the disaster: April 25th, 2015
- Location of the survey (Lat. Lon., name or address): Kathumandu, SunKoshi, Melamchi, Dhunche
- Date of the field survey (if any): May 27th to June 2nd, 2015
- Survey tools (if any): Laser ranger, GPS receiver
- Key findings: Creeping mountain slopes, local soil subsidence, peak discharges in monsoon rains

Key Words : *Gorkha Earthquake, geotechnical problems, Monsoon rains*

1. INTRODUCTION

The April 2015 Nepal earthquake of Mw=7.8 (USGS), also known as the Gorkha earthquake, was the worst natural disaster to strike Nepal since the 1934 Nepal–Bihar earthquake. As of May 26th, the police report had confirmed 8,664 fatalities, with more than 21,954 injured (Source: Japan Embassy in Nepal). The quake was followed by many aftershocks including the one of M=7.3 that struck north-eastern Nepal on Tuesday, May 12th. Among the areas of most concern are those where soil/rock masses detached from slopes have fallen into rivers, posing an ongoing menace that will be likely to increase when seasonal monsoon rains begin to fall in June. This report outlines the findings obtained through the reconnaissance of the JSCE Landslide survey group, JSCE/ Japanese Geotechnical Society (JGS)/ Japan Association for Earthquake Engineering (JAEE) Joint Investigation Team for the 2015 Nepal Earthquake Disaster.

2. LANDSLIDES AND MONSOON RAINS

The earthquake bears comparison with the 1923 Great Kanto earthquake, Japan, in terms of its moment magnitude of 7.9, though there have been various opinions on its magnitude ranging from 7.9 to 8.3[1)]. As it was one of serious post-earthquake problems in the 1923 Great kanto earthquake, so landslides and debris flows will certainly be a serious impact to not only millions of people, who lost their mountain homes, huddling in the monsoon rains, but also civil-infrastructures along rivers such as intake facilities of hydro-power stations, bridges, etc.

"Landslides triggered by the 25 April Nepal earthquake were mapped by experts at the British Geological Survey, Durham University, and a volunteer group coordinated by Jet Propulsion Laboratory (JPL) - NASA, the University of Arizona, and International Center for Integrated Mountain Development (ICIMOD), and are provided in the ArcGIS geodatabase format on webpages in references 2), 3) and 4).

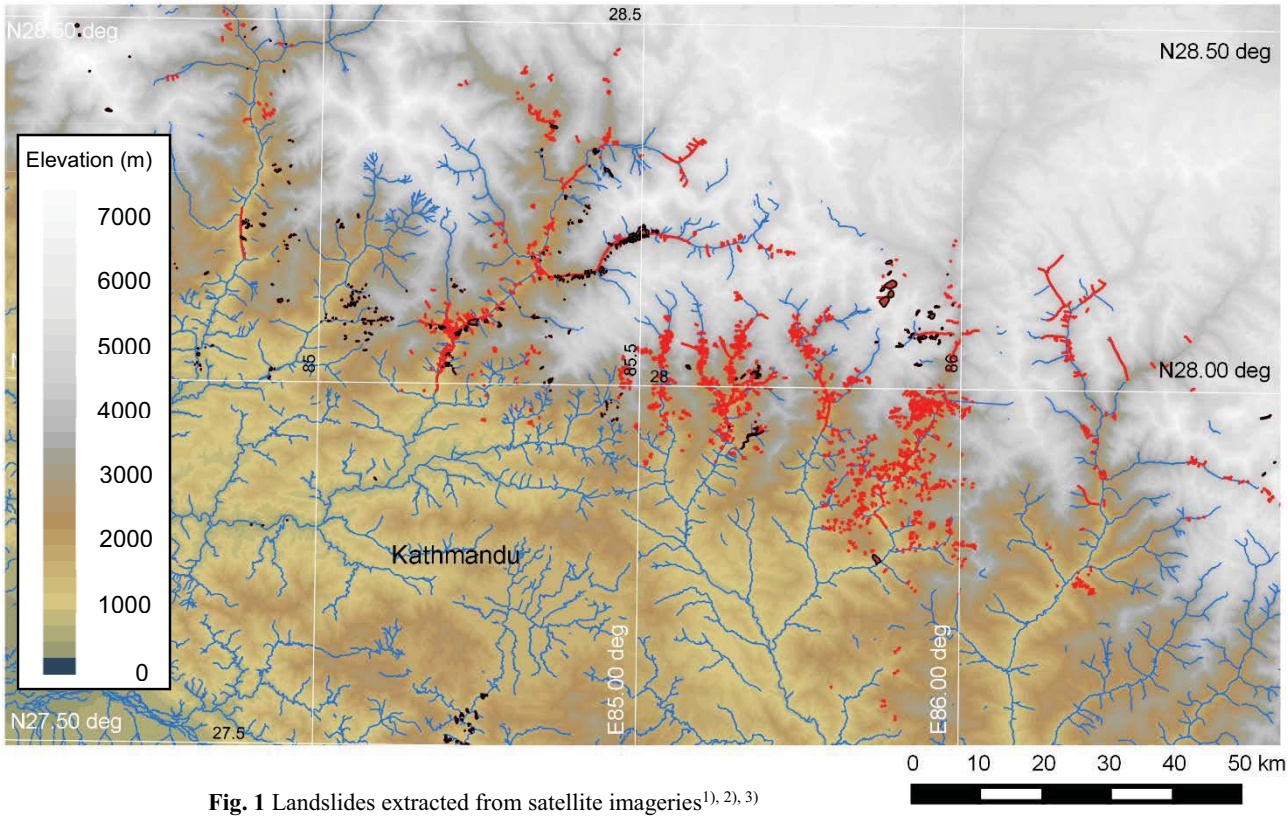

Fig. 1 Landslides extracted from satellite imageries[1), 2), 3)]

Satellite data used to prepare this data set include those from the International Charter Space and Major Disasters, as well as freely-available online viewers. Maps for the authors' survey were prepared given this set of digital data (Fig. 1). Note that the dataset was last updated on May 8th, 4 days before the largest Mw=7.3 aftershock of May 12.

(1) Estimation of peak discharge in monsoon

Since one of the major post-quake concerns is the increase in discharge of river water in the upcoming rainy season, a rough and ready estimation of peak discharges was made at 2 points along the Sunkoshi River (Table 1), where a large landslide mass is clogging its stream as will be discussed in the following section.

River water depth h is first estimated by observing hydraulic disturbances transmitted downstream within a steady cone of apex angle θ (Fig. 2)

$$v_{jump} = \sqrt{gh} = v_{flow} \cdot \sin\theta \qquad (1)$$

where, g = gravitational acceleration, and v_{flow} = observed flow velocity. Manning's empirical equation[5)] is then used to calculate Manning coefficient of roughness n at the chosen points:

$$v_{ave} = \frac{1}{n} R^{2/3} i^{1/2} \qquad (2)$$

where v_{ave} = cross-sectional average velocity (m/s) which is tentatively assumed to be 2/3 of the observed peak flow velocity v_{flow}, R = hydraulic radius (m) and i = slope of the hydraulic grade line. Though it may be a mere coincidence that the estimated

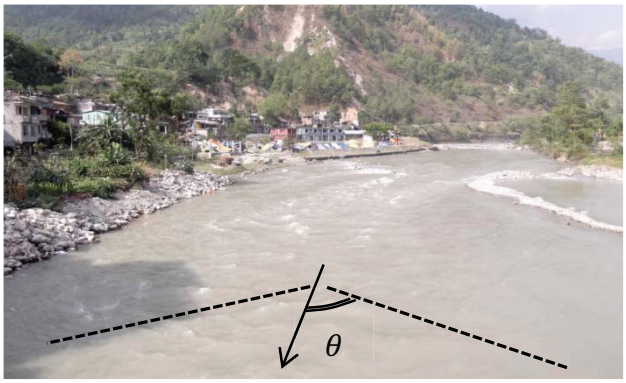

Fig. 2 Hydraulic jump propagating across flow at an angle θ at Point 2 (N27.75387°, E85.82750°). The distortion of angle θ in the photo is corrected.

Table 1 Locations of chosen points

Point Number	Longitude	Latitude
1	E85.88150°	N27.81655°
2	E85.82750°	N27.75387°

roughness coefficient values n are about the same with each other, these values lie in ranges recommended by the Japan Ministry of Land, Infrastructure, Transport and Tourism (MLIT) for mountain river beds covered up with gravel ($0.030 < n < 0.050$) and big boulders ($0.040 < n$). Therefore the average value of $n = 0.045$ is used to estimate both current and peak discharges. To estimate peak discharges, the peak water depths are estimated based on eyewitness accounts (Table 3).

Table 2 Manning's roughness coefficients n estimated at two points along Sun Koshi river

Point No.	Observed flow velocty (m/s)	Angle at which wave propagates across flow (deg)	Velocity of Hydraulic jump (m/s)	Estimated maximum depth (m)	River bed drop (m)	over Distance (m)	River bed inclination	Hydraulic radius (m)	Average flow velocity (m/s)	Estimated Gauckler–Manning coefficient
	v_{flow}	θ	$v_{jump} = v_{flow} \cdot \sin\theta$	$D_{max} = {v_{jump}}^2/g$	Δh	L	$i = \Delta h/L$	$R \cong 2 \times D_{max}/3$	$v_{ave} \cong 2 \times v_{flow}/3$	$n = R^{2/3} i^{1/2}/v_{ave}$
1	3	45	2.12132034	0.459184	5	128.6	0.0388802	0.30612245	2	0.044781432
2	2.9	70	2.7251086	0.757777	4.6	232.4	0.0197935	0.50518482	1.93333333	0.046158779

Table 3 Estimated current (May 28, 2015) and peak discharges (m^3/s)

Point No.	Effective river water width (m)	water cross-section (m^2)	Current discharge	Credible increase of river water level (m)	Increase in river width (m)	Credible maximum river-water cross section	Credible peak velocity	Credible peak discharge
		$A \cong W \times D_{max}/2$	$Q_{current} \cong v_{ave} \times A$					
1	30	6.887755102	13.7755102	2	2	73.79591837	7.685783	567.17942
2	28	10.60888126	20.5105038	2	20	120.2488715	5.622115	676.05298

Peak average velocities of 7.7 to 5.6 m/s associated with the estimated peak discharges of 500 to 700 m^3/s may occur in the rainy season, which velocities can be substantially large for the river-bed load including large boulders to be eroded as can be predicted by the Hjulström curve[6] shown in Appendix A.

(2) Sunkoshi landslide mass

Heavy rainfall on August 2, 2014 triggered a landslide on a steep valley wall of metamorphic rock of Sunkoshi river (Fig. 3) The landslide mass reportedly killed 156 people and blocked the river to form a lake behind it. Though the landslide was not caused by the earthquake, the presence of the landslide mass that has fallen in the river will certainly have an important and serious effect on the riverbed load transport and thus important facilities such as intake gates for hydropower stations. It is reported by the Earth Observatory, NASA that some 5.5 million cubic meters of rock and debris tumbled down into the Sunkoshi River valley[7]. A 3D image of the exposed slip surface was made to see more details of detached and deposited rock and debris using Epipolar geometry[8], which geometry allows a 3D image from photos taken from different locations to be reconstructed. Though three photos were taken from three different Points 1, 2 and 3 (Table 4), Points 2 and 3 are a little too close to each other. Therefore one more reference point (Point 4) was taken, for better control of positioning, at an exposed rock on the intact mountain slope, which can be seen from all the camera locations. The longitude, latitude and elevation of this point were tentatively obtained from a Landsat imagery and the 30m SRTM DEM (Shuttle Radar Topography Mission Digital Elevation Model)[9].

The obtained digital elevation model for the exposed slip surface of Sunkoshi is shown in Fig. 4. Though the entire stretch of the exposed surface was not completely covered, there are a clear hollow of the top source region, major triple-terraced cliffs on the top, halfway up and near the toe of the exposed surface with conic talus deposits (collections of broken rock fragments) rimming along the bases of these cliffs. The angle of repose for these talus deposits varies from 15 for low-lying coarse rock deposits to 30 degrees for high-lying finer granular deposits.

Fig. 3 Sunkoshi Landslide
(Photo by K. Konagai taken at N27.761312, E85.875274, on May 28th, 2015)

The 30m SRTM DEM[9] was used herein as the terrain model before the landslide event, and compared with the obtained digital elevation model of the exposed slip surface. Fig. 5 shows the change in elevation within the measured slip surface area.

The volumes of the detached and deposited masses are estimated to be 11.6 million m^3 and 3.9 million m^3 respectively. The observed area is not covering the major part of the soil mass that has fallen into the river, and the remaining mass of 7.7 million m^3 may

Table 4 Reference points for reconstructing 3D image

Point No.	Longitude (degree)	Latitude (degree)	UTM value easting, *x* (m)	UTM value northing, *y* (m)	Elevation (m)
1	85.869678	27.755511	388609.86	3070631.27	896.535034
2	85.876536	27.76144	389291.83	3071281.94	893.824341
3*	85.875274	27.761312	389167.33	3071268.88	864.986816
4	85.869813	27.772017	388640	3072460	1380

* Coordinates of Point 3 were not used for geo-referencing.

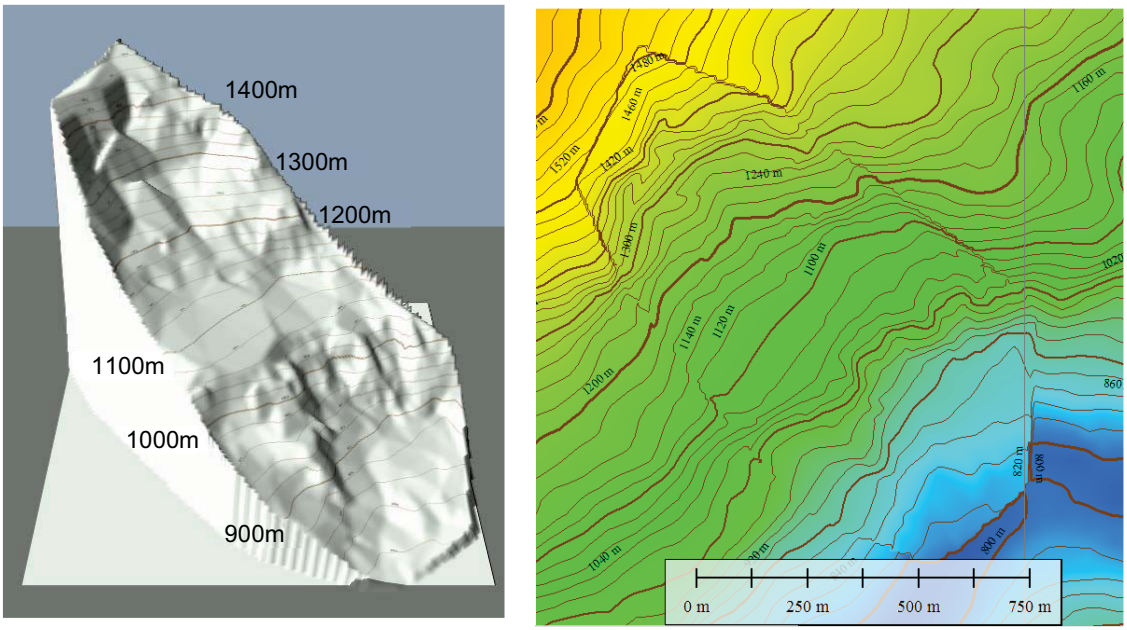

Fig. 4 DEM of slip surface of Sunkoshi Landslide

be as much as the rock/debris volume of 5.5 million m^3 estimated by NASA[6]. However, the estimated volumes are sensitive to points taken for geo-referencing (Table 4). Revised values will be reported in future publications.

(3) Creeping landslide mass

According to eyewitness accounts, an about 1.5 km long soil mass was first detached in the heavy rain season of 2002 from the zone of about 2100m ASL on a high mountain slope, and fell along a deeply incised gulley down to Trishuli river about 1300m below the exposed scar to clog the stream. A temporary road was quickly constructed across this zone for the important traffic of Trishuli road leading to Dhunche not to be suspended long.

However, the road started moving inch by inch towards the toe. Fig. 6 shows two satellite images of the zone from different times, the upper and lower ones from May 3, 2015 and January 4, 2010, respectively. It is noted in the latest 2015 photo that the temporary road section crossing the landslide zone is currently west of the location where this section used to be in 2010, indicating that this section

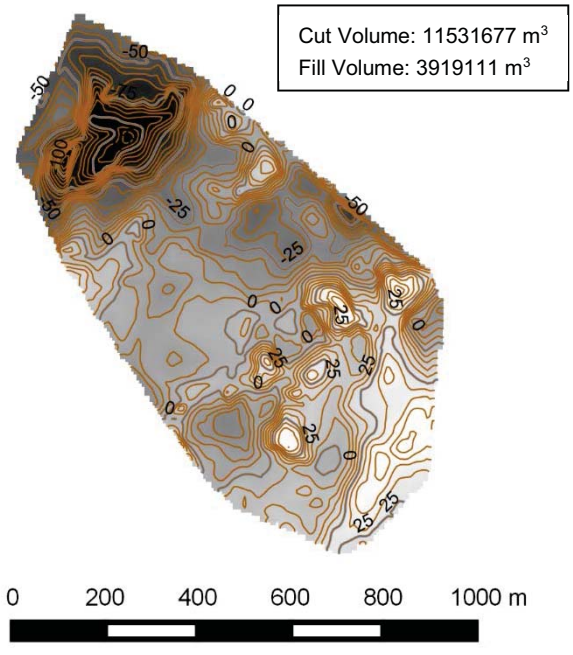

Fig. 5 Change in elevation within exposed slip surface

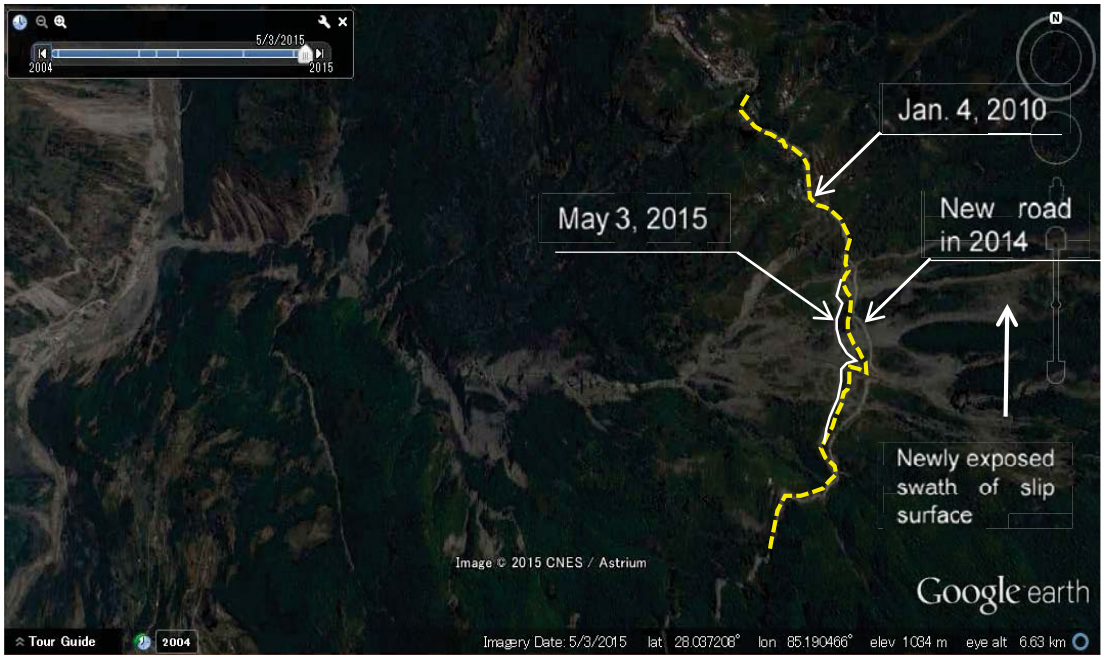

(a) Landslide zone on May 3rd, 2015

(b) Landslide zone on January 4th, 2010

Fig. 6 Landslide zone (Satellite images taken from Google Earth)

has been carried down the slope over about 30m horizontal distance. Moreover swaths of bare slip surfaces above the temporary road, which swaths were not visible in the 2010 photo, are appearing and becoming thicker year by year. Though the earthquake had reportedly invisible and indirect effect upon the remaining landslide mass, the movement of the mass can be further accelerated in the upcoming rainy season of 2015.

All along the Trishuli road from this point of continuous creeping to Dhunche, clear indications of dilating landslide masses can be seen from place to place. Fig. 7 shows a pair of photographs of a dilating debris mass, which was cut at this elevation for the temporary road construction. These photos, arranged side by side can be perceived as a single image in terms of depth, and one notices that the matrix of fine sand filling up the voids of sub-angular rocks/ boulders exhibits fresh open cracks, an indication that the fabric of these embedded large rocks are slowly dilating.

Fig. 7 Sign of dilating debris mass halfway up on a landslide mass, which was cut at this elevation for the temporary road construction at N28.067959°, E85.228808° (Photo by K. Konagai)

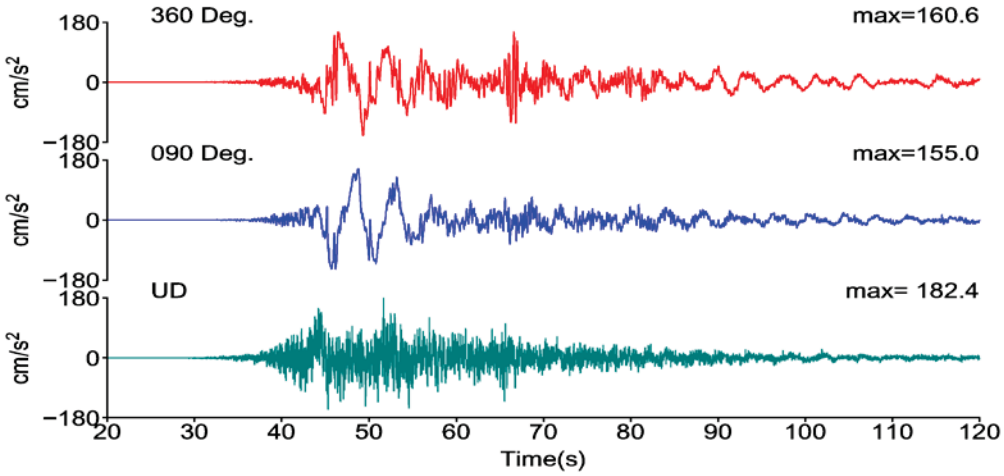

Fig. 8 Three orthogonal components of acceleration time history observed at USGS- NSMP strong groundmotion station in Kathmandu at N27.7120°, E85.3160° [10)]

3. KATHMANDU CITY

(1) Clusters of damaged houses/ buildings

One interesting preliminary observation was the unusual nature of the earthquake motion recorded at the Kanti Path strong-motion station, Kathmandu, of the National Strong Motion Project (NSMP), United States Geological Survey (USGS)[10)], which record exhibited a long predominant period of around 5 s (Fig. 8). Though the peak ground accerelations in the east-west and north-south directions were about 0.16G at most, this fact indicated that the ground motion at this station was very slow with overall ground displacements of over a meter, as opposed to the quick series of jolts that we often observe in ordinary earthquakes. This may be attributed to the fact that the city in the Kathmandu basin spreads over an about 550 m thick deposit of Paleo Kathmandu Lake, which deposit is considered to be of Pliocene to Pleistocene in age[11)].

However, this motion may not necessarily represent the motions particularly in areas most seriously hit by this earthquake. The GDACS (Global Disaster Alert and Coordination System) LIVE map[4)], which integrates geo-spatial data from a range of sources in support to response efforts following the Gorkha earthquake, shows that seriously damaged houses and buildings were clustered very locally along rims of terraces and valleys of streams that cut the terraces down to a little lower elevations. When these damaged houses and buildings are mapped upon the PALSAR II interferogram[12)], it is noted that the biggest cluster of damaged houses/ buildings can be found where the east-west trending parallel firinge pattern shows some clear disturbance (Area 1 in Fig. 9). This disturbance can be considered to be a local deformation of the ground. There is not necessarily a clear causual relationship confirmed between the local ground deformation and the cluster of damaged

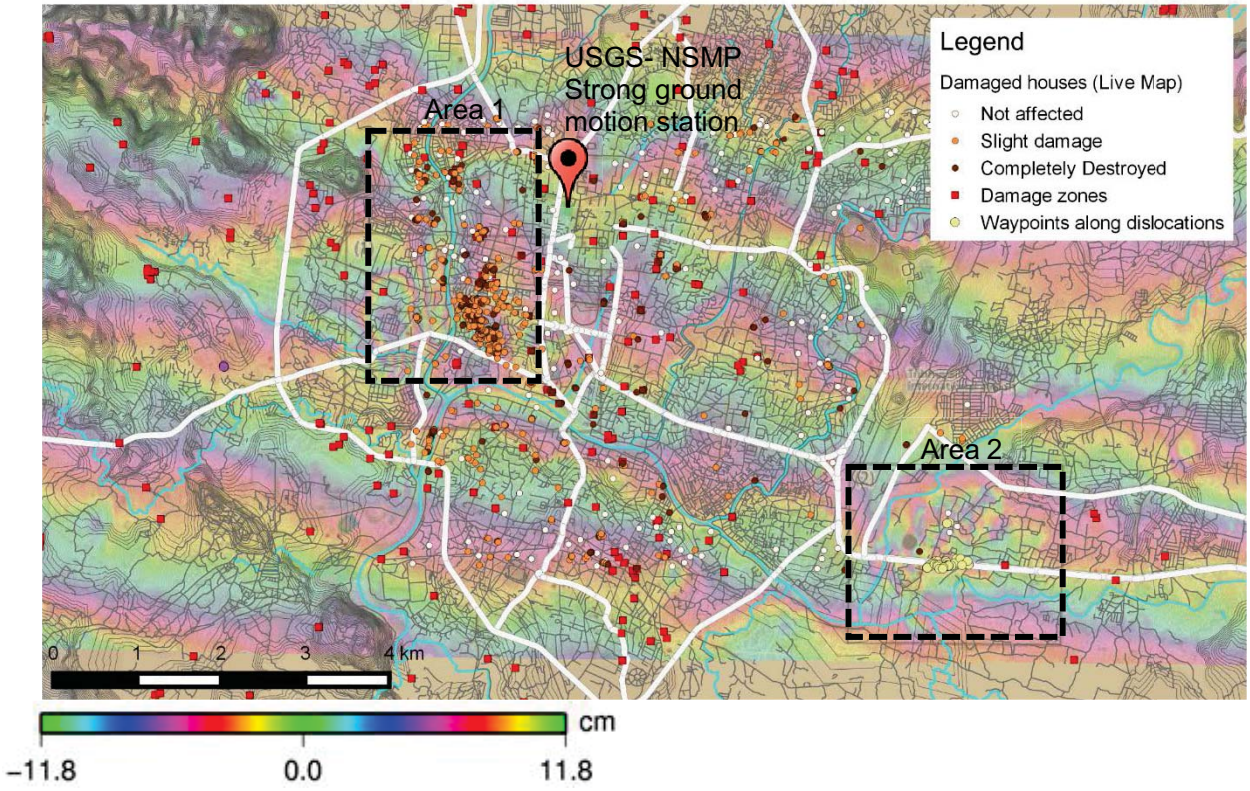

Fig. 9 Distribution of damaged houses/ buildings on GDACS Live map derived from satellite imagery and field data, and PALSAR II interferogram[12] showing some disturbances in Areas 1 and 2.

houses/ buildings. However, the ground motion here may have been intense enough to cause both the ground deformation and the damage to houses/ buildings though the sequence of these two are not clear yet.

(2) Depressed section of Araniko Highway

One more disturbance of the fringe pattern of PALSAR 2 interferogram (Area 2 in Fig. 9) can be found about 2 km southeast of the Kathmandu International Airport. One segment of the Kathmandu-Bhaktapur Road section of the Araniko Highway goes across this area. Several lines of vertical ground dislocations appeared diagonally across this road making up a 200m wide swath of ground failure. Way points were marked along visible dislocation lines by a GPS receiver as shown in Fig. 10. The observed ground dislocation lines are about parallel to each other trending in NEE to SWW direction and curving slightly north. These lines die out beyond their eastern and western ends, and about 300 to 400 m long at the most, indicating that the failure was just localized within this short extent of the swath. Two outermost lines of relatively large dislocation indicates that the area between these two major dislocation lines has sunken by about 2m.

However the midmost lines suggest that the lowest wet zone may have been pushed slightly up. To highlight this feature of mass movement, a longitudinal section of the highway was measured by using a handy laser-ranger (Fig. 10).

Though the cause of this ground depression is yet controversial, a local lateral spread of hill slopes towards the low-lying wet ground is considered to have been responsible for this failure. The wet and slightly depressed area along a small creek may have been liquefied and/or weakened enough to allow the hillsides on both sides of the creek to move a little sideways against each other, and bulged. This ground depression was responsible for the deformation of a two-span continuous pedestrian overpass, whose north pier rests exactly on the south-easternmost line of dislocation while the other two are on the relatively intact hill terrace. As the result, the northern pier was on an outward tilt, causing the joint between the pier and the deck to open up by about 40 to 45 cm. It was lucky that the deck of the overpass did not fall onto the highway probably because it was a two-span continuous beam. However there could have been a good chance for any single supported deck of overpass to fall upon the highway with its spans expanded. According to one of our members who have been there on May 2nd, the joint may have been opened a little wider (Fig. 11), indicating that the tilt of the pier has been increasing gradually and/or in a step-wise manner over a month's period since the earthquake hit.

Given the above findings, local soil conditions are

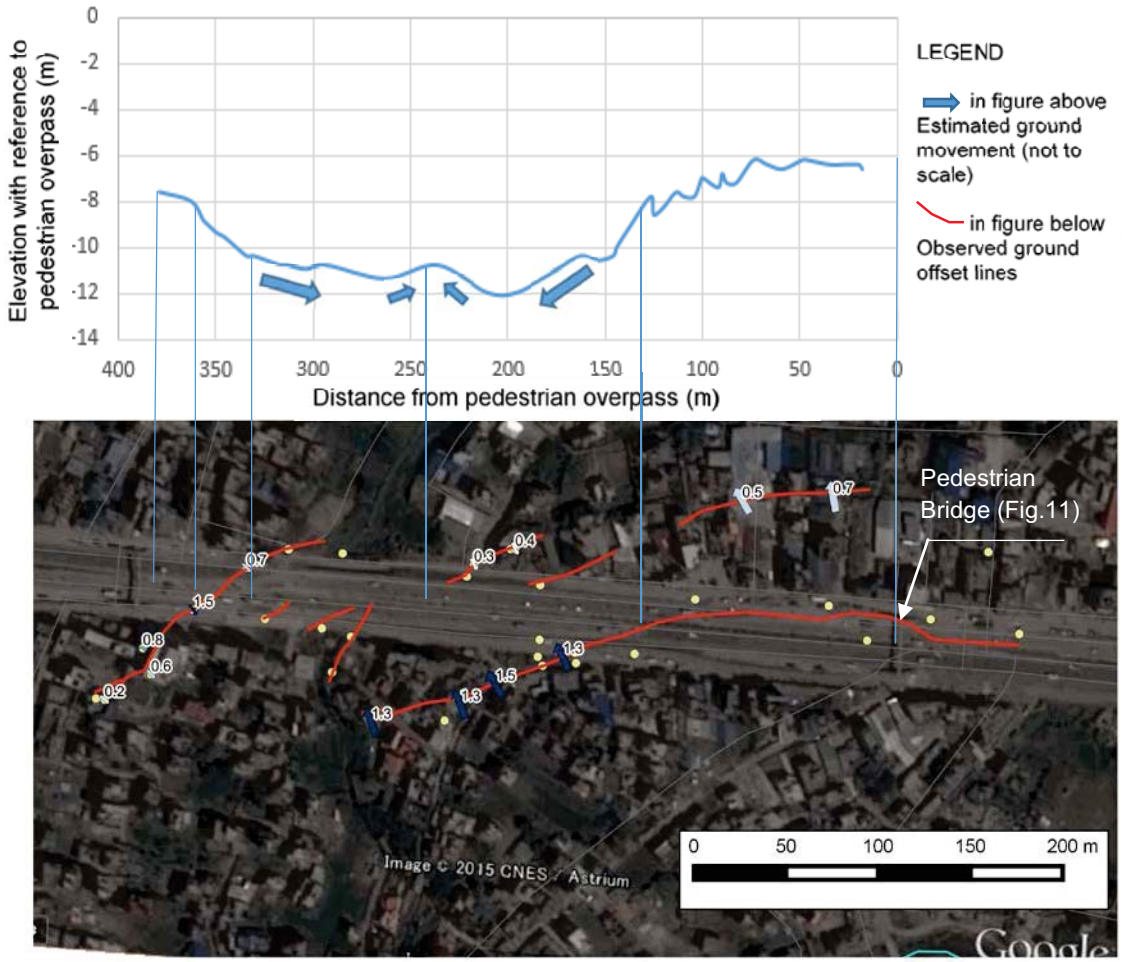

Fig. 10 Depressed section of Araniko Highway and ground offsets in Area 2 (Photo from Google Earth)

Fig. 11 Joint opened between deck and pier of the pedestrian overpass. Photos left and right by R. Pokhrel on May 2nd and 31st, 2015, respectively, at N27.674601°, E85.364705°: Assuming that the notch depth *D* of the pier-top landing for the bridge-girder seating is the same for both photos of May 2nd and May 31st, these photos are suggestive that the joint has opened a little wider over a month's period.

to be carefully reflected upon rehabilitation plans in a rational manner, because as has been frequently seen in the past earthquakes, it can take months for liquefied/weakened soil to regain its initial strength, and even after it regains the strength, the soil can remain susceptible to re-liquefaction in a next big earthquake. To pinpointing locations of weak soils, InSAR imageries may be useful as shown in Fig. 9.

4. RECOMMENDATIONS

It has been reported that the population of Kathmandu grows by 6.5 percent each year[13], and much of the city's existing housing stock was constructed before building codes were first drafted in 1993 to 1994 and approved in 2003[14]. However the findings through this survey indicated that local geological/ geotechnical conditions may have been also responsible for serious destructions, which were clustered densely in some particular areas. Unstable mountain slopes that exhibit some creeping movements and landslide masses that have fallen into rivers pose an ongoing menace that is likely to increase in the monsoon rains. In this kind of situation, and given the pledgement in the donner conference of June 25 that 4.4 billions of dollars will

be given to help rebuild this earthquake-ravaged nation[15], no delay is allowed in mapping out rational tactics for better rehabilitations. Here follow the recommendations based upon what the authors found through their reconnaissance:

(1) Continuous monitoring of creeping slopes from satellites is important. Once early signs of accelerated movements are found, pin-point countermeasures can be taken in a quick and rational manner.

(2) Peak discharge and associated riverbed load transportation rate are to be estimated based upon much more reliable information. This estimation is particularly important to deal with potential risks for intake facilities of hydropower stations, etc.

(3) Volumes and dimensions of large landslide masses clogging major streams are also to be estimated.

(4) Something that should not be forgotten in discussing rehabilitation strategies is that a large earthquake often causes long lasting geotechnical problems. Once liquefied and/or weakened, soil can remain soft for months. Locations with similar land deformations to the depressed section of Araniko Highway are to be identified and their causes are to be thoroughly studied to reflect the natures of weak soils upon rehabilitation/ reconstruction plans.

ACKNOWLEDGMENT: Special thanks of the authors go to Mr. Masashi Ogawa, Ambassador, Mr. Shinya Machida, Counsellor, and Mr. Makoto Oyama, First Secretary at the Embassy of Japan, Kathmandu, Nepal, who have provided the authors with briefing of the earthquake-induced damage, and organized an information exchange meeting among Japanese reconnaissance teams.

APPENDIX A HJULSTRÖM CURVE

The Hjulström diagram[6] (Fig. A1) has been widely used to determine whether a river would erode, transport, or deposit riverbed sediment probably because it is very easy to use. The upper and lower curves in Hjulström diagram show the critical flow velocity for riverbed errosion and the deposition velocity, respectively, as a function of particle size. Later, Sundborg[16] modified Hjulström diagram to show separate curves of the critical flow velocities for several water depths. In any versions of this diagram, flow velocities reaching 6 to 7 m/s is substantially large for the river-bed load including large boulders to be eroded.

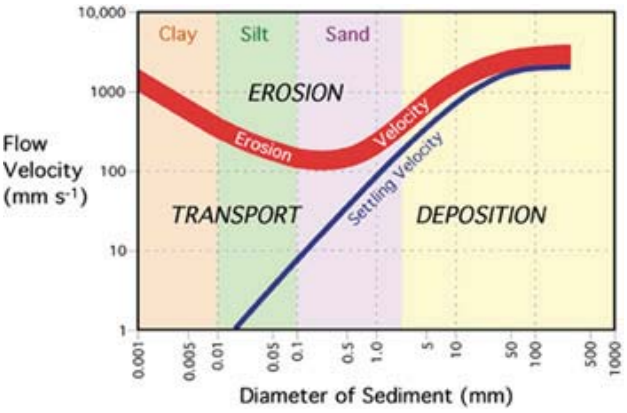

Fig. A1 Hjulström diagram (retrieved from Ref. 17))

REFERENCES

1) Usami T.: Mterials for comprehensive list of destructive earthquakes in Japan, University of Tokyo Press, 2003.
2) Durham University / BGS Team, Nepal earthquake landslide locations, 8 May 2015, https://data.hdx.rwlabs.org/dataset/lands https://data.hdx.rwlabs.org/dataset?q=Nepal+earthquake+landslide+locations%2C+8+May+2015
3) Durham / BGS Team, Nepal: UPDATED (28 May) landslide inventory following 25 April Nepal earthquake, etc., http://ewf.nerc.ac.uk/blog/
4) UNITAR-UNOSAT: GDACS LIVE map, Earthquake, Nepal, EQ-2015-000048-Nepal, https://www.arcgis.com/apps/webappviewer/index.html?id=b9f9da798f364cd6a6e68fc20f5475eb
5) Manning R.: On the flow of water in open channels and pipes. Transactions of the Institution of Civil Engineers of Ireland, 20, 161-207, 1891.
6) Hjulstrom, F.: Studies of the morphological activity of rivers as illustrated by the River Fyris. Bulletin of the Geological Institute University of Uppsala, 25, 221-527, 1935.
7) NASA Earth Observatory, Before and After the Sunkosi Landslide, http://earthobservatory.nasa.gov/NaturalHazards/view.php?id=84406
8) SolidFromPhoto 32, http://www.solidfromphoto.sakura.ne.jp/
9) The humanitarian Data Exchange, Central Nepal Digital Elevation Model (DEM), https://data.hdx.rwlabs.org/dataset/9cdbade9-fca2-4d23-99ab-9f3a396ae929/resource/f895e259-17da-4973-a8fb-97f8628e8e63
10) Center for Engineering Strong Motion Data (CESMD), Cooperative effort of USGS, CGS and ANSS, http://strongmotioncenter.org/
11) Pandey M. R.: Ground response of Kathmandu valley on the basis of microtremors, 12th World Conference on Earthquake Engineering, Paper No. 2106, Auckland, New Zealand, http://www.iitk.ac.in/nicee/wcee/article/2106.pdf
12) Earth Observation Research Center, Japan Aerospace Exploration Agency, ALOS-2/PALSAR-2 Observation Results of the 2015 Nepal Earthquake (4), http://www.eorc.jaxa.jp/ALOS-2/en/img_up/dis_pal2_npl-eq_20150502.htm
13) Pradhan P. K.: Population Growth, Migration and Urbanisation. Environmental Consequences in Kathmandu Valley, Nepal, Environmental Change and its Implications

for Population Migration, Advances in Global Change Research Vol. 20, 177-199, 2004. http://link.springer.com/chapter/10.1007%2F978-1-4020-2877-9_9
14) EERI Nepal Earthquake Clearing House, Nepal National Building Code (NBC): An Overview, http://www.eqclearinghouse.org/2015-04-25-nepal/2015/05/05/nepal-national-building-code-nbc-an-overview/
15) Thalif Deen (United Nations): Donors Pledge Over 4.4 Billion Dollars to Nepal - But With a Caveat, http://www.globalissues.org/news/2015/06/26/21171
16) Sundborg, A.: The River Klarålven: Chapter 2. The morphological activity of flowing water—erosion of the stream bed: Geografiska Annaler, Vol. 38, 165-221, 1956.
17) University of Bristol, Questionmark Perception, June 30, 2015, https://qmp.bris.ac.uk/perception5/open.php?SESSION=9126309306926432&NAME=Tutor&GROUP=ESU

(Received July 1st, 2015)